Polarization analysis of χ_{cJ} decay into octet baryonic pairs*

Cai-Ying Pang (庞彩莹)[1] Rong-Gang Ping (平荣刚)[2,4†] Dai-Hui Wei (魏代会)[3,1‡]

[1]School of Physical Science and Technology, Guangxi Normal University, Guilin 541004, China
[2]Institute of High Energy Physics, Chinese Academy of Sciences, Beijing 100049, China
[3]Guilin Normal College, Guilin 541199, China
[4]University of Chinese Academy of Sciences, Chinese Academy of Sciences, Beijing 100049, China

Abstract: This work presents a comprehensive analysis of polarization transfer in the decays of χ_{cJ} $(J=0,1,2)$ into octet baryon-antibaryon pairs in polarized electron-positron collisions. Using the spin density matrix formalism, we trace the polarization from the initial beams through the production chain $e^+e^-\to\psi(2S)\to\gamma\chi_{cJ}$ to the final-state baryon-antibaryon system. The helicity amplitude analysis for $\chi_{c1}\to B\bar{B}$ confirms the universal angular distribution parameter $\alpha=-1/3$, as dictated by the charge-conjugation helicity selection rule. For χ_{c2} decays, α and the transverse polarization depend on two independent amplitudes, and our quark-model calculations agree with existing data. We demonstrate that the longitudinal beam polarization P_z modifies the spin observables for χ_{c1} and χ_{c2}. This offers new experimental handles at future polarized facilities, such as the Super τ-Charm Facility (STCF), to test decay mechanisms and explore baryonic spin entanglement as a quantum information resource.

Keywords: polarization, *P*-wave charmonia, baryon, spin density matrix

DOI: 10.1088/1674-1137/ae8004 **CSTR:** 32044.14.ChinesePhysicsC.50103101

I. INTRODUCTION

The study of charmonium physics provides a unique window into both perturbative and nonperturbative aspects of Quantum Chromodynamics (QCD). Among the charmonium states, the P-wave triplet χ_{cJ} $(J=0,1,2)$ holds particular interest due to its intermediate mass scale, where the interplay between the production dynamics, governed by perturbative QCD (pQCD), and the subsequent hadronization into final-state hadrons, a nonperturbative process, can be intricately probed. The decay channels $\chi_{cJ}\to B\bar{B}$, where B denotes a spin-1/2 baryon such as proton, neutron, or Λ, are especially valuable in this regard. These decays involve the creation of a baryon-antibaryon pair from a colorless, heavy quark-antiquark system, offering a testing ground for models of hadron formation, helicity conservation rules, and the role of higher-order QCD effects [1−3]. Understanding the detailed decay mechanism of χ_{cJ} whether dominated by short-distance pQCD diagrams, influenced by non-relativistic QCD (NRQCD) matrix elements, or affected by rescattering and final-state interactions remains an active area of theoretical investigation. The polarization observables in these decays are particularly sensitive to the underlying dynamics, as they trace the transfer of angular momentum from the initial quarkonium state to the final-state baryons [4−7].

Experimentally, significant progress has been made in measuring the branching fractions and angular distributions of $\chi_{cJ}\to B\bar{B}$ decays. Facilities such as the BESIII experiment at the Beijing Electron Positron Collider (BEPCII) have produced large and clean samples of χ_{cJ} particles via the radiative transition $\psi(2S)\to\gamma\chi_{cJ}$. Recent analyses have provided precise measurements of the branching fractions for channels like $\chi_{cJ}\to p\bar{p}$, $\Sigma^0\bar{\Sigma}^0$, $\Sigma^+\bar{\Sigma}^-$, $\Xi^-\bar{\Xi}^+$ and $\Xi^0\bar{\Xi}^0$ [8−13]. Notably, these measurements reveal a distinct hierarchy in the decay rates among the different χ_{cJ} states and significant angular distribution parameters (α parameters) for the baryons, which are directly linked to the polarization transfer. The experimental data, with ever-increasing precision, pose both challenges and opportunities for theoretical models, calling for a more refined description that goes beyond the simplest pQCD or statistical hadronization pictures.

The polarization of the final-state baryons and the related phenomenon of spin entanglement constitute a fron-

Received 8 March 2026; Accepted 22 June 2026; Accepted manuscript online 23 June 2026
* Supported by the National Natural Science Foundation of China (NSFC) (12575112, 12465015)

† E-mail: pingrg@ihep.ac.cn
‡ E-mail: weidh@gxnu.edu.cn

tier in quantum information aspects of particle physics [14−16]. In the decay $\chi_{cJ} \to B\bar{B}$, the spin-1/2 baryon and antibaryon pair is produced in a quantum-correlated state. For the χ_{c1} and χ_{c2} decays, the initial state possesses nonzero spin alignment, which can lead to a non-trivial spin density matrix for the baryon-antibaryon system. This entanglement, a direct consequence of quantum mechanics and angular momentum conservation, can be quantified through observables like spin correlations and entanglement entropy [17, 18]. Recent theoretical works have begun to explore these quantum correlations in heavy quarkonium decays, suggesting that such processes could serve as high-energy laboratories for testing fundamental quantum principles [19−21]. However, most existing analyses assume an unpolarized initial χ_{cJ} state, typically produced from unpolarized e^+e^- collisions. The role of the initial production mechanism in shaping the final spin correlations remains less explored.

In this work, we extend the polarization analysis of $\chi_{cJ} \to B\bar{B}$ decays, with B representing octet baryon, to a more general and experimentally relevant scenario: the production of χ_{cJ} from the annihilation of polarized electron and positron beams. Polarized beam experiments, such as those possible at future e^+e^- colliders like the STCF [22] or upgraded BEPCII, offer an additional handle to control and manipulate the initial angular momentum state. By considering polarized initial beams, we introduce a new axis of quantization and a controllable source of spin alignment for the χ_{cJ} meson. This allows us to study how the beam polarization propagates through the production process $(e^+e^- \to \psi(2S) \to \gamma\chi_{cJ})$ and subsequently transfers to the final-state baryons via the decay $\chi_{cJ} \to B\bar{B}$. We systematically calculate the complete set of helicity amplitudes for these processes within a quark-model framework, incorporating both the production and decay dynamics. Our analysis aims to predict the resulting baryon spin polarizations and spin correlations as functions of the beam polarization parameters. We quantify the expected experimental observables, such as angular distributions and polarization correlation, and discuss how measurements of these observables with polarized beams could provide unprecedented constraints on the χ_{cJ} decay mechanism, test helicity selection rules with greater discriminative power, and offer new insights into the spin entanglement properties of the baryon-antibaryon system. This study bridges the gap between traditional charmonium spectroscopy and the emerging field of high-energy quantum information, highlighting the potential of polarized colliders as powerful tools for fundamental QCD studies.

II. SPIN DENSITY MATRIX

A. $\psi(2S)$ particle

In e^+e^- colliders, the laboratory coordinate system is conventionally defined with the z-axis aligned along the beam direction, typically chosen as the momentum direction of the positron (e^+). The x-axis is usually set perpendicular to the beam axis within the accelerator plane, and the y-axis completes the right-handed Cartesian system (as shown in Fig. 1). When the electron beams possess both longitudinal and transverse polarizations, the spin density matrix (SDM) for the initial e^+e^- system must account for these polarization states. For an electron with longitudinal polarization P_z and transverse polarization $\vec{P}_t = (P_x, P_y) = P_T e^{i\phi_e}$, with ϕ_e the azimuthal angle, its individual spin density matrix can be expressed as $\rho_e = \frac{1}{2}(I + \vec{P}\cdot\vec{\sigma})$, where $\vec{P} = (P_x, P_y, P_z)$ and $\vec{\sigma}$ are the Pauli matrices. The combined SDM for the colliding e^+e^- pair is then the direct product of their individual matrices: $\rho_{e^+e^-} = \rho_{e^+} \otimes \rho_{e^-}$.

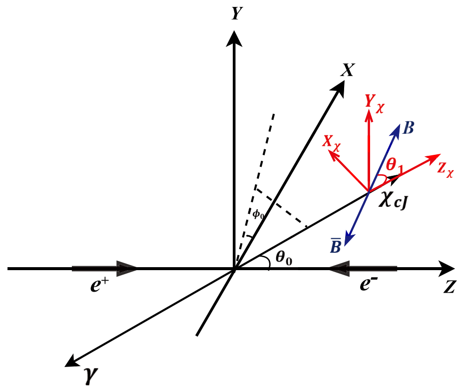

Fig. 1. (color online) Definition of the helicity system and helicity angles for the decays $\psi(2S) \to \gamma\chi_{cJ}$ and $\chi_{cJ} \to B\bar{B}$.

In the process $e^+e^- \to \psi(2S)$, assuming helicity conservation and parity conservation in the coupling via a virtual photon, the helicity of the virtual photon is restricted to $\lambda_\gamma = \pm 1$. The SDM for the produced $\psi(2S)$ can then be derived from the decay matrix formalism. The general relation is $\rho_f = M\rho_i M^\dagger$, where ρ_i is the SDM of the initial e^+e^- system, and M is the decay amplitude matrix for $e^+e^- \to \gamma^* \to \psi(2S)$, expressed in terms of helicity amplitudes and Wigner D-functions. For the specific case discussed in this paper, which focuses on the longitudinal polarization $P_z(\bar{P}_z)$ of the e^- and e^+ beams, the transverse polarization P_T of both beams also arises from the self-polarization due to the Sokolov-Ternov effect [23]. Thus one has the SDM for $\psi(2S)$ particle:

$$\rho^{\gamma*/\psi(2S)} = \frac{1}{2}\begin{pmatrix} (1+\bar{P}_z)(1-P_z) & 0 & P_T^2 \\ 0 & 0 & 0 \\ P_T^2 & 0 & (1-\bar{P}_z)(1+P_z) \end{pmatrix}. \quad (1)$$

At the $\psi(2S)$ production energy, the transverse polarization P_T in BEPCII reaches 0.28 after one hour of beam injection, in accordance with the Sokolov-Ternov mechanism, which predicts a characteristic rise time of $\tau_0 = 2.8$ hours [24]. The polarization magnitude increases with beam energy under identical injection conditions, illustrating the energy-dependent build-up of polarization.

B. χ_{cJ} states

In the decay $\psi(2S)(\lambda) \to \chi_{cJ}(\lambda_1)\gamma(\lambda_2)$, the helicity angle θ_0 is defined as the angle between the χ_{cJ} momentum and the positron direction in the $\psi(2S)$ rest frame, and the azimuthal angle is denoted by ϕ_0. The helicity amplitudes $A^{(J)}_{\lambda_1,\lambda_2}$ give the decay amplitude for specific helicity states λ_1 (of χ_{cJ}) and λ_2 (of γ), where λ_i denotes the spin projection along the particle's momentum direction.

This charmonium transition conserves parity, leading to specific symmetry relations among the helicity amplitudes. For the χ_{c0} final state, the amplitudes satisfy $A^{(0)}_{0,-1} = A^{(0)}_{0,1}$. In the case of χ_{c1}, the relations are $A^{(1)}_{-1,-1} = -A^{(1)}_{1,1}$ and $A^{(1)}_{0,-1} = -A^{(1)}_{0,1}$. For χ_{c2}, the amplitudes follow $A^{(2)}_{-2,-1} = A^{(2)}_{2,1}$, $A^{(2)}_{-1,-1} = A^{(2)}_{1,1}$, and $A^{(2)}_{0,-1} = A^{(2)}_{0,1}$. These constraints arise from parity conservation and the spin properties of the final states [25].

The helicity amplitude $A^{(J)}_{\lambda_1,\lambda_2}$ encodes the dynamical information of the transition $\psi(2S) \to \chi_{cJ}\gamma$. Theoretical arguments and BESIII measurements confirm that this process is dominated by electric dipole (E1) transitions [26]. Consequently, the helicity amplitudes follow E1 selection rules[27]: for χ_{c1}, $A^{(1)}_{1,1} = A^{(1)}_{0,1}$; for χ_{c2}, $A^{(2)}_{2,1} = \sqrt{2}A^{(2)}_{1,1} = \sqrt{6}A^{(2)}_{0,1}$. These relations reflect the angular momentum and parity constraints of E1 transitions. The SDM of χ_{cJ} can be expressed as a linear transformation of the $\psi(2S)$ SDM:

$$\rho(\chi_{cJ}) = M\rho^{\gamma*/\psi(2S)}M^{\dagger}, \quad \text{with}$$
$$M_{\lambda,\lambda_1-\lambda_2} = \mathcal{N}_J D^1_{\lambda,\lambda_1-\lambda_2}(\phi_0,\theta_0,0)A^{(J)}_{\lambda_1,\lambda_2}. \tag{2}$$

Here, $\mathcal{N}_J$ is a normalization factor, and $D^1_{i,j}$ denotes the Wigner D-matrix element. Note that the polarization parameters P_T and P_z depend on the azimuthal angle ϕ_0. The elements of $\rho(\chi_{cJ})$ can be written as $\rho_{\lambda_1,\lambda_1'}(\chi_{cJ}) \propto \sum_{\lambda,\lambda',\lambda_2} \rho^{\psi(2S)}_{\lambda,\lambda'} D^1_{\lambda,\lambda_1-\lambda_2}(\Omega_0) D^{1*}_{\lambda',\lambda_1'-\lambda_2}(\Omega_0) \times A^{(J)}_{\lambda_1,\lambda_2}A^{(J)*}_{\lambda_1',\lambda_2}$, where $\lambda,\lambda' = \pm1$ denote the helicities of the $\psi(2S)$ produced in e^+e^- annihilation, and $\lambda_2 = \pm1$ corresponds to the photon helicity. This expression explicitly shows how the polarization components of the $\psi(2S)$, encoded in $\rho^{\psi(2S)}_{\lambda\lambda'}$, are mapped onto the χ_{cJ} states through the radiative transition.

Combining Eq. (1) and Eq. (2), and using the E1 selection rules, the angular distribution of the χ_{cJ} particle is obtained by taking the trace of its SDM

$$\frac{\mathrm{d}\sigma}{\mathrm{d}\cos\theta_0\mathrm{d}\phi_0} \propto \begin{cases} 1 & \text{for } \chi_{c0}, \\ \dfrac{1}{2}\left[(1-\bar{P}_zP_z)(5-\cos 2\theta_0) - 2P_T^2\cos 2\phi_0 \sin^2\theta_0\right]|A_{0,1}|^2 & \text{for } \chi_{c1}, \\ \dfrac{1}{12}\left[(1-\bar{P}_zP_z)(27+\cos 2\theta_0) + 2P_T^2\cos 2\phi_0 \sin^2\theta_0\right]|A_{2,1}|^2 & \text{for } \chi_{c2}. \end{cases} \tag{3}$$

One can see that the ϕ_0 distribution depends on P_T, which provides a means to measure the beam transverse polarization. Moreover, if the positron is unpolarized, the $\cos\theta_0$ distribution is independent of the electron polarization. For unpolarized beams ($\bar{P}_z = P_z = P_T = 0$), the angular distribution reduces to $\mathrm{d}\sigma/\mathrm{d}\cos\theta_0 \propto 1+\alpha\cos^2\theta_0$, with $\alpha = 0, -1/3, 1/13$ for χ_{c0}, χ_{c1}, and χ_{c2} [28], respectively.

From Eq. (2), it is evident that the spin density matrix of χ_{cJ} depends on the helicity angles θ_0 and ϕ_0. To investigate the polarization effects in the subsequent decay $\chi_{cJ} \to B\bar{B}$ through baryon angular distributions, we adopt the momentum-space averaged SDM of χ_{cJ}. This is obtained by integrating over θ_0 and ϕ_0, effectively marginalizing the angular dependence. If E1 approximation is assumed, one has the normalized SDM of χ_{c1}

$$\mathcal{N}_1\rho(\chi_{c1}) = \begin{pmatrix} -16(-1+\bar{P}_zP_z) & -3\sqrt{2}\pi(\bar{P}_z-P_z) & 0 \\ -3\sqrt{2}\pi(\bar{P}_z-P_z) & -32(-1+\bar{P}_zP_z) & -3\sqrt{2}\pi(\bar{P}_z-P_z) \\ 0 & -3\sqrt{2}\pi(\bar{P}_z-P_z) & -16(-1+\bar{P}_zP_z) \end{pmatrix}, \tag{4}$$

where the normalization factor $\mathcal{N}_1 = 64(1-\bar{P}_zP_z)$. For the χ_{c2} state, one has the normalized SDM

$$\mathcal{N}_2\rho(\chi_{c2}) = \begin{pmatrix} -96(1-\bar{P}_zP_z) & 18\pi(-\bar{P}_z+P_z) & -8\sqrt{6}(1-\bar{P}_zP_z) & 0 & 0 \\ 18\pi(-\bar{P}_z+P_z) & -48(1-\bar{P}_zP_z) & -3\sqrt{6}\pi(\bar{P}_z-P_z) & 0 & 0 \\ -8\sqrt{6}(1-\bar{P}_zP_z) & -3\sqrt{6}\pi(\bar{P}_z-P_z) & -32(1-\bar{P}_zP_z) & -3\sqrt{6}\pi(\bar{P}_z-P_z) & -8\sqrt{6}(1-\bar{P}_zP_z) \\ 0 & 0 & -3\sqrt{6}\pi(\bar{P}_z-P_z) & -48(1-\bar{P}_zP_z) & 18\pi(-\bar{P}_z+P_z) \\ 0 & 0 & -8\sqrt{6}(1-\bar{P}_zP_z) & 18\pi(-\bar{P}_z+P_z) & -96(1-\bar{P}_zP_z) \end{pmatrix}. \tag{5}$$

The normalization factor $\mathcal{N}_2 = 320(-1+\bar{P}zP_z)$. The averaged SDM then serves as input for analyzing the $B\bar{B}$ decay angular correlations, where the initial χ_{cJ} polarization is imprinted on the final-state baryon pair. This approach isolates the intrinsic polarization transfer from the χ_{cJ} production dynamics, independent of the $\psi(2S)\to\chi_{cJ}\gamma$ kinematic configuration.

C. $B\bar{B}$ pair

In the decay process $\chi_{cJ}(\lambda_1)\to B(\lambda_3)\bar{B}(\lambda_4)$, we investigate polarization effects in the helicity frame of the $B\bar{B}$ system. The helicity frame is defined in the center-of-mass frame of the χ_{cJ}. In this frame, the baryon and antibaryon are emitted back-to-back. The momentum direction of the baryon is chosen as the Z_B-axis of the $B\bar{B}$ helicity frame. The Y_B-axis is taken to be perpendicular to the plane spanned by the momenta of the χ_{cJ} and the baryon, while the X_B-axis is defined such that (X_B,Y_B,Z_B) forms a right-handed coordinate system, as illustrated in Fig. 1. In this frame, the helicity amplitude of the $B\bar{B}$ pair is denoted by $B^J_{\lambda_3,\lambda_4}$, and the spin density matrix of the $B\bar{B}$ system can be expressed as:

$$\begin{aligned}&\rho^{(J)}(BB) = M\rho(\chi_{cJ})M^\dagger, \ \text{with}\\ &M_{\lambda_1,\lambda_3-\lambda_4} = D^J_{\lambda_1,\lambda_3-\lambda_4}(\phi_1,\theta_1,0)B^{(J)}_{\lambda_3,\lambda_4},\end{aligned} \tag{6}$$

where $J=0,1$ and 2 for χ_{c0},χ_{c1} and χ_{c2} states.

For the decay $\chi_{cJ}\to B\bar{B}$, parity conservation implies the following relations for the helicity amplitudes [25]: $B^{(J)}_{-\lambda_3,-\lambda_4} = (-1)^J B^{(J)}_{\lambda_3,\lambda_4}$, which gives $B^{(0,2)}_{-\lambda_3,-\lambda_4} = B^{(0,2)}_{\lambda_3,\lambda_4}$ for $\chi_{c0,2}$, $B^{(1)}_{-\lambda_3,-\lambda_4} = -B^{(1)}_{\lambda_3,\lambda_4}$ for χ_{c1}. In addition, the charge conjugation symmetry requires $B^{(1)}_{\lambda_3,\lambda_4} = -B^{(1)}_{\lambda_4,\lambda_3}$, so that $B^{(1)}_{-1/2,-1/2} = B^{(1)}_{1/2,1/2} = 0$. Consequently, only the amplitudes $B^{(1)}_{-1/2,1/2}$ and $B^{(1)}_{1/2,-1/2}$ contribute to the decay $\chi_{c1}\to B\bar{B}$, with the relation $B^{(1)}_{-1/2,1/2} = -B^{(1)}_{1/2,-1/2}$. This helicity selection rule implies that the helicity amplitude for $\chi_{c1}\to B\bar{B}$ is governed by a single parameter. For the χ_{c2} decay, the two independent amplitudes are parameterized by their phase difference Δ: $B^{(2)}_{-\frac{1}{2},\frac{1}{2}} = e^{i\Delta}B^{(2)}_{\frac{1}{2},\frac{1}{2}}$.

1. $\chi_{c0}\to B\bar{B}$

With these relations, the SDM for χ_{c0} decays can be expressed in the helicity basis.

$$\rho^{(0)}(B\bar{B}) = \frac{1}{2}\begin{pmatrix} 1 & 0 & 0 & 1 \\ 0 & 0 & 0 & 0 \\ 0 & 0 & 0 & 0 \\ 1 & 0 & 0 & 1 \end{pmatrix}. \tag{7}$$

It follows that the baryon angular distribution is isotropic in the $B\bar{B}$ helicity frame.

2. $\chi_{c1}\to B\bar{B}$

While for χ_{c1} decay, the SDM of the $B\bar{B}$

$$\rho^{(1)}(B\bar{B}) \propto \begin{pmatrix} 0 & 0 & 0 & 0 \\ 0 & \rho_{22} & \rho_{23} & 0 \\ 0 & \rho_{32} & \rho_{33} & 0 \\ 0 & 0 & 0 & 0 \end{pmatrix}, \tag{8}$$

with

$$\begin{aligned}\rho_{22} =& 2\left[2(\bar{P}_zP_z-1)(\cos 2\theta_1-5)\right.\\ &\left.+3\pi(P_z-\bar{P}_z)\cos\phi_1\sin\theta_1\right]|B_{\frac{1}{2},-\frac{1}{2}}|^2,\\ \rho_{33} =& 2\left[2(\bar{P}_zP_z-1)(\cos 2\theta_1-5)\right.\\ &\left.+3\pi(\bar{P}_z-P_z)\cos\phi_1\sin\theta_1\right]|B_{\frac{1}{2},-\frac{1}{2}}|^2,\\ \rho_{23} =& \rho_{32} = 8(1-\bar{P}zP_z)\sin^2\theta_1|B_{\frac{1}{2},-\frac{1}{2}}|^2.\end{aligned} \tag{9}$$

It follows that the baryon angular distribution in the $B\bar{B}$ helicity frame is expressed

$$I^{(1)}(\theta_1) \propto (1-\bar{P}_zP_z)(5-\cos 2\theta_1)|B_{\frac{1}{2},-\frac{1}{2}}|^2. \tag{10}$$

The angular distribution is given by $1-\frac{1}{3}\cos^2\theta_1$, a form independent of the beam polarization.

3. $\chi_{c2}\to B\bar{B}$

After the integration over ϕ_1, the SDM of $B\bar{B}$ for χ_{c2} decays

$$\rho^{(2)}(B\bar{B}) \propto \begin{pmatrix} 2\mathrm{e}^{\mathrm{i}\Delta}(3c_{2\theta}-7)b_{++}^2 & \sqrt{6}s_{2\theta}b_{+-}b_{++} & -\sqrt{6}s_{2\theta}b_{+-}b_{++} & 2\mathrm{e}^{\mathrm{i}\Delta}(3c_{2\theta}-7)b_{++}^2 \\ \sqrt{6}\mathrm{e}^{2\mathrm{i}\Delta}s_{2\theta}b_{+-}b_{++} & 3\mathrm{e}^{\mathrm{i}\Delta}(c_{2\theta}-5)b_{+-}^2 & -6\mathrm{e}^{\mathrm{i}\Delta}s_\theta^2 b_{+-}^2 & \sqrt{6}\mathrm{e}^{2\mathrm{i}\Delta}s_{2\theta}b_{+-}b_{++} \\ -\sqrt{6}\mathrm{e}^{2\mathrm{i}\Delta}s_{2\theta}b_{+-}b_{++} & -6\mathrm{e}^{\mathrm{i}\Delta}s_\theta^2 b_{+-}^2 & 3\mathrm{e}^{\mathrm{i}\Delta}(c_{2\theta}-5)b_{+-}^2 & -\sqrt{6}\mathrm{e}^{2\mathrm{i}\Delta}s_{2\theta}b_{+-}b_{++} \\ 2\mathrm{e}^{\mathrm{i}\Delta}(3c_{2\theta}-7)b_{++}^2 & \sqrt{6}s_{2\theta}b_{+-}b_{++} & -\sqrt{6}s_{2\theta}b_{+-}b_{++} & 2\mathrm{e}^{\mathrm{i}\Delta}(3c_{2\theta}-7)b_{++}^2 \end{pmatrix} \cdot (\bar{P}_z Pz-1)\mathrm{e}^{-\mathrm{i}\Delta}, \qquad (11)$$

where $c_{2\theta}=\cos 2\theta_1$, $s_{2\theta}=\sin 2\theta_1$, $s_\theta=\sin\theta_1$, $b_{++}=|B_{1/2,1/2}|$, $b_{+-}=|B_{1/2,-1/2}|$, and Δ is the phase angle difference between $B_{1/2,-1/2}$ and $B_{1/2,1/2}$.

It follows that the baryon's angular distribution in the $B\bar{B}$ helicity frame is

$$I^{(2)}(\theta_1) \propto (1-\bar{P}_z P_z)(1+\alpha\cos^2\theta_1) \quad \text{with}$$
$$\alpha = -\frac{3b_{+-}^2+6b_{++}^2}{9b_{+-}^2+10b_{++}^2}. \qquad (12)$$

Note that in the approximation of the E1 transition, the angular distribution is independent of the $\cos^4\theta_1$ term.

III. POLARIZATION $B\bar{B}$ IN χ_{cJ} DECAYS

Spin entanglement between baryon pairs is a paradigmatic manifestation of non-classical correlations in spin systems and has become an important resource in quantum physics. It not only provides a crucial experimental platform for testing the foundations of quantum mechanics—such as Bell nonlocality and local realism—but is also emerging as a sensitive quantum probe for detecting new physics. Within this framework, spin polarization serves as an ideal physical carrier for realizing and manipulating baryonic entanglement, making its preparation and measurement techniques central to experimental research. For a two-body spin-1/2 system, its quantum information can be fully described by the polarization vectors of the baryon, O_i, and of the antibaryon, $\bar{O}_j$ $(i,j=x,y,z)$, and the second-order spin correlation tensor $C_{ij}=\langle\sigma_i\otimes\sigma_j\rangle$. In terms of Pauli matrices, the spin density matrix for $B\bar{B}$ reads

$$\rho^{(J)}(B\bar{B}) = \frac{1}{4}\Big[\mathbf{I}\otimes\mathbf{I}+\sum_i O_i(\sigma_i\otimes\mathbf{I}) + \sum_j \bar{O}_j(\mathbf{I}\otimes\sigma_j)+\sum_{ij}C_{ij}\sigma_i\otimes\sigma_j\Big], \qquad (13)$$

where $\mathbf{I}$ denotes the 2×2 identity matrix.

On the other hand, the polarization vector and the correlation tensor can be expressed if the SDM is available, with

$$O_i = \mathrm{Tr}[\rho^{(J)}(B\bar{B})\sigma_i\otimes\mathbf{I}],$$
$$\bar{O}_j = \mathrm{Tr}[\rho^{(J)}(B\bar{B})\mathbf{I}\otimes\sigma_i],$$
$$C_{ij} = \mathrm{Tr}[\rho^{(J)}(B\bar{B})\sigma_i\otimes\sigma_j]. \qquad (14)$$

1. $\chi_{c0}\to B\bar{B}$

Using the SDM for $\chi_{c0}\to B\bar{B}$ as given by Eq. (7), we obtain the polarization vectors $O_i=\bar{O}_i=0\ (i=x,y,z)$ for the baryon and antibaryon. The spin correlation matrix C_{ij}, defined in Eqs. (13), (14), reads:

$$C = \begin{pmatrix} 1 & 0 & 0 \\ 0 & -1 & 0 \\ 0 & 0 & 1 \end{pmatrix}. \qquad (15)$$

The decay $\chi_{c0}\to B\bar{B}$ is of particular interest for quantum information studies. For a bipartite $B\bar{B}$ system described by the density matrix $\rho^J(B\bar{B})$, the entanglement of formation is quantified by the concurrence $C[\rho]$ [29]. Following the standard definition, $C[\rho]=\max(0,t_1-t_2-t_3-t_4)$, where t_i are the square roots of the eigenvalues of $R=\rho(\sigma_y\otimes\sigma_y)\rho^*(\sigma_y\otimes\sigma_y)$ sorted in descending order. Using the joint spin density matrix $\rho^{(0)}(B\bar{B})$, we find $C[\rho]=1$ for the χ_{c0} decay, implying that the χ_{c0} state is maximally entangled [17].

2. $\chi_{c1}\to B\bar{B}$

Using the SDM for $\chi_{c1}\to B\bar{B}$, one obtains the polarization vectors $O_i=\bar{O}_i=0\ (i=x,y)$ and $O_z=-\bar{O}_z=\dfrac{\rho_{33}-\rho_{22}}{\rho_{22}+\rho_{33}}$ for the baryon and antibaryon. Note that the longitudinal polarization is useful for measuring the subsequent decay of the hyperon. The spin correlation matrix C_{ij} defined in Eqs. (13), (14) reads

$$C = \frac{1}{\rho_{22}+\rho_{33}}\begin{pmatrix} \rho_{23}+\rho_{32} & \mathrm{i}(\rho_{32}-\rho_{23}) & 0 \\ \mathrm{i}(\rho_{23}-\rho_{32}) & \rho_{23}+\rho_{32} & 0 \\ 0 & 0 & -1 \end{pmatrix}. \qquad (16)$$

Here, $\rho_{ij}(i,j=1,2,3)$ are the SDM elements of the $B\bar{B}$ for χ_{c1} decay, as given by Eq. (9).

3. $\chi_{c2} \to B\bar{B}$

For $\chi_{c2} \to B\bar{B}$, using Eq. (11), the polarization vectors for the baryon and antibaryon are obtained as $O_i = \bar{O}_i = 0$ $(i = x, z)$, and

$$O_y = -\bar{O}_y = \frac{1}{\mathcal{F}}(4\sqrt{6}\cos\theta_1 \sin\theta_1 \sin\Delta b_{+-} b_{++}). \tag{17}$$

The spin correlation matrix reads

$$C_{11} = \frac{1}{\mathcal{F}}[2(3\cos 2\theta_1 - 7)b_{++}^2 - 3(1-\cos 2\theta_1)b_{+-}^2], \tag{18}$$

$$C_{22} = \frac{1}{\mathcal{F}}[2\left(7 - 3\cos 2\theta_1\right)b_{++}^2 - 6\sin^2\theta_1\, b_{+-}^2], \tag{19}$$

$$C_{33} = \frac{1}{\mathcal{F}}[-3(\cos 2\theta_1 - 5)b_{+-}^2 + 2(3\cos 2\theta_1 - 7)b_{++}^2], \tag{20}$$

$$C_{31} = -C_{13} = \frac{1}{\mathcal{F}}[4\sqrt{6}\cos\Delta\cos\theta_1 \sin\theta_1\, b_{+-} b_{++}], \tag{21}$$

$$C_{12} = C_{21} = C_{23} = C_{32} = 0, \tag{22}$$

with

$$\mathcal{F} = 3(\cos 2\theta_1 - 5)b_{+-}^2 + 2(3\cos 2\theta_1 - 7)b_{++}^2.$$

IV. HELICITY AMPLITUDE IN QUARK MODEL

We compute the helicity amplitudes for $\chi_{c2} \to B\bar{B}$ using the conventional constituent quark model [30–32]. At tree level (see Fig. 2), the $c\bar{c}$ pair in the χ_{c2} annihilates into two gluons, which subsequently convert into two $q\bar{q}$ pairs and combine with an additional $q\bar{q}$ pair (with 0^{++} quantum numbers) produced from the QCD vacuum. The three (anti)quarks then hadronize into (anti)baryons, forming the final-state baryon-antibaryon pair. As an approximation, only the contribution of the baryon wave function at the origin in momentum space is taken into account; that is, the momentum of each constituent quark is taken as a fixed fraction of the baryon momentum, weighted by the mass of the quark that constitutes the baryon.

In estimating the angular distribution coefficients for $\chi_{c2} \to B\bar{B}$ using helicity amplitudes, the decay mechanism described by the constituent quark model at tree level can be further simplified. Considering Eq. (12), the angular distribution coefficients are determined by the ratios of helicity amplitudes. The QCD nonperturbative effects introduced by the initial- and final-state hadron wave functions, as well as common color factors, cancel out in these ratios, leaving only the dependence on the helicities of the quark pairs. These ratios of helicity amplitudes constitute the primary factor in determining the angular distribution coefficients. The helicity amplitudes for the decay $\chi_{c2} \to B\bar{B}$ can be written as

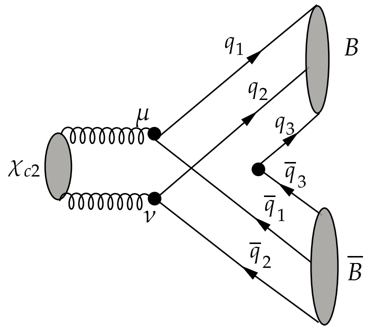

Fig. 2. χ_{c2} decays into a baryon-antibaryon pair.

$$\begin{aligned} b_{\lambda_3,\lambda_4} =& F\langle\Psi_B\Psi_{\bar{B}}|\bar{u}(\lambda_1)\gamma^\mu v(\bar{\lambda}_1)\bar{u}(\lambda_2)\gamma^\nu v(\bar{\lambda}_2)\bar{u}(\lambda_3)v(\bar{\lambda}_3) \\ &+ (u\leftrightarrow s) + (d\leftrightarrow s)|\epsilon_{\mu\nu}(\lambda_3-\lambda_4)\rangle, \end{aligned} \tag{23}$$

where F is an overall constant that accounts for the initial- and final- state hadron wave functions at the origin, as well as the color factor. Here $u(v)$ denotes the free Dirac spinor for a quark (antiquark), Ψ_B ($\Psi_{\bar{B}}$) is the spin wave function of the baryon (antibaryon), including the spin $\chi_B(\chi_{\bar{B}})$ and flavor wave functions (ϕ_B), and $\epsilon_{\mu\nu}(\lambda_3-\lambda_4)$ represents the spin wave function of the χ_{c2} with helicity $\lambda_3-\lambda_4$. Their explicit expressions of wave functions are given in appendix. In the constituent quark model, we parameterize nonperturbative QCD effects, including hadronic bound states and long-distance effects, into a single overall constant. Their values can be determined from the measured decay width. However, they cancel out in the calculation of helicity amplitude ratios.

We calculate the amplitude in the $B\bar{B}$ helicity system, where the spin quantization axis (Z-axis) is chosen along the baryon momentum direction, placing the antibaryon along the $-Z$ axis. The explicit spinor solutions in the Pauli-Dirac representation are given for a particle of mass m, energy E, and momentum along or opposite to the z-axis. For helicity $\lambda = \pm 1/2$ states, the baryon spinors are:

$$\begin{aligned} u(p_z, \pm 1/2) &= \left(\sqrt{E+m}\chi_\pm \pm \sqrt{E-m}\chi_\pm\right), \\ u(-p_z, \pm 1/2) &= \left(\sqrt{E+m}\chi_\mp \pm \sqrt{E-m}\chi_\mp\right), \end{aligned} \tag{24}$$

and the antibaryon spinors are:

$$v(p_z, \pm 1/2) = \left(\sqrt{E-m}\chi_{\mp} \mp \sqrt{E+m}\chi_{\mp}\right),$$
$$v(-p_z, \pm 1/2) = \left(-\sqrt{E-m}\chi_{\pm} \pm \sqrt{E+m}\chi_{\pm}\right), \quad (25)$$

with two-component basis spinors $\chi_+ = (1,0)^T$ and $\chi_- = (0,1)^T$.

Using these equations, one obtains

$$\bar{u}(P_q, 1/2)v(-P_q, 1/2) = -2P_q,$$
$$\bar{u}(P_q, 1/2)\not{\epsilon}(0)v(-P_q, 1/2) = -2m_q,$$
$$\bar{u}(P_q, 1/2)\not{\epsilon}(1)v(-P_q, -1/2) = -2\sqrt{2}E_q, \quad (26)$$

where P_q is the momentum magnitude for the quark q with mass m_q and energy E_q. The polarization vectors are taken as $\epsilon(\pm 1) = \mp\frac{1}{\sqrt{2}}(0,1,\pm \mathrm{i},0)^T$ and $\epsilon(0) = (0,0,0,1)^T$.

Then the helicity amplitude for $\chi_{c2} \to B\bar{B}$ is calculated as follows:

$$b_{+,+}(N\bar{N}) = -4\sqrt{\frac{2}{3}}P_q\left(\frac{10}{3}m_q^2 - \frac{8}{9}E_q^2\right),$$
$$b_{+,-}(N\bar{N}) = -\frac{80}{9}E_q m_q P_q,$$
$$b_{+,+}(\Lambda\bar{\Lambda}) = -8\sqrt{\frac{2}{3}}P_q\left(2m_q m_s - P_q P_s\right),$$
$$b_{+,-}(\Lambda\bar{\Lambda}) = -16E_s m_q P_q,$$
$$b_{+,+}(\Sigma\bar{\Sigma}) = -\frac{8}{3}\sqrt{\frac{2}{3}}(2(E_q^2 + 3m_q^2) + (12m_s m_q - 8E_s E_q)P_q),$$
$$b_{+,-}(\Sigma\bar{\Sigma}) = \frac{32}{3}(2E_q(m_q P_s + m_s P_q) - E_s m_q P_q),$$
$$b_{+,+}(\Xi\bar{\Xi}) = -\frac{8}{3}\sqrt{\frac{2}{3}}(E_s^2 P_q - 4E_q E_s P_s + 3m_s(P_q m_s + 2m_q P_s)),$$
$$b_{+,-}(\Xi\bar{\Xi}) = \frac{16}{3}(-E_q m_s P_s + 2E_s(P_q m_s + m_q P_s)). \quad (27)$$

Here $N\bar{N}$ denote proton-antiproton $p\bar{p}$ or neutron-antineutron $n\bar{n}$, $\Sigma\bar{\Sigma}$ denote $\Sigma^0\bar{\Sigma}^0$ or $\Sigma^+\bar{\Sigma}^-$, $\Xi\bar{\Xi}$ denote $\Xi^0\bar{\Xi}^0$ or $\Xi^-\bar{\Xi}^+$. The m_u, m_d, E_u, E_d are the masses and energies of u and d quarks. Under the assumption $m_u = m_d = m_q$ and $E_u = E_d = E_q$, the light-quark momentum is $P_q = \sqrt{E_q^2 - m_q^2}$. Correspondingly, for the strange quark (mass m_s, energy E_s), we have $P_s = \sqrt{E_s^2 - m_s^2}$.

In the numerical evaluation of helicity amplitudes, the light-quark mass is set to $m_q = m_p/3 = 0.31$ GeV [33], and the strange-quark mass is determined via $m_s = (m_\Lambda - m_p) + m_q$ GeV, where m_Λ denotes the Λ-baryon mass, yielding $m_s = 0.49$ GeV. Quark momenta are obtained as $P_q = m_q P_B/M$ and $P_s = m_s P_B/M$, with $M = m_u + m_d + m_s$ being the total quark mass and P_B the baryon momentum. We estimate the corresponding uncertainty by evaluating our results at $m_s = 0.43$ GeV and 0.53 GeV, and quote the larger difference as the uncertainty. Numerical results for the decays $\chi_{c2} \to B\bar{B}$ are listed in Table 1. Due to the adoption of the $m_u = m_d$ assumption, the processes for the Ξ^- and Ξ^0 are treated unified. The calculated angular distribution parameters agree with the experimental data within one standard deviation.

V. POLARIZATION OBSERVABLE

A. Angular distribution

In the decay processes χ_{cJ} to spin-1/2 baryon antibaryon pair, the polar angular distribution of the final-state baryon in the helicity frame provides a direct probe into the parent particle's polarization and the underlying helicity amplitudes. The angular distribution can be generally expressed as $I(\theta_1) \propto 1 + \alpha\cos^2\theta_1$. For the scalar state χ_{c0}, the parameter α is predicted to be zero, resulting in a flat, isotropic distribution, a direct consequence of its $J = 0$ nature, which forbids any spin alignment. In contrast, for the axial-vector χ_{c1}, the decay into any octet baryon-antibaryon pair is governed by a helicity selection rule enforced by charge conjugation symmetry. This rule strictly constrains the helicity amplitudes, leading to a model-independent prediction of $\alpha = -1/3$ for all such

Table 1. Numerical helicity amplitudes and angular distribution parameters for the χ_{c2} decay into octet baryonic pairs. α denotes the numerical estimate, while α(Exp) represents the measured values.

Channel	b_{+-}	b_{++}	α	α(Exp)
$p\bar{p}$	-0.816 ± 0.001	-0.016 ± 0.001	-0.333 ± 0.001	-0.26 ± 0.17 [9]
$n\bar{n}$	-0.816 ± 0.001	-0.016 ± 0.001	-0.333 ± 0.001	-
$\Lambda\bar{\Lambda}$	-1.488 ± 0.191	-0.177 ± 0.016	-0.337 ± 0.001	$-0.211 \pm 0.100 \pm 0.050$ [11]
$\Sigma^0\bar{\Sigma}^0$	2.762 ± 0.221	-0.438 ± 0.153	-0.341 ± 0.007	-
$\Sigma^+\bar{\Sigma}^-$	2.762 ± 0.221	-0.438 ± 0.153	-0.341 ± 0.007	-
$\Xi^-\bar{\Xi}^+$	1.824 ± 0.409	-0.461 ± 0.121	-0.351 ± 0.006	$-0.34 \pm 0.18 \pm 0.30$ [13]
$\Xi^0\bar{\Xi}^0$	1.824 ± 0.409	-0.461 ± 0.121	-0.351 ± 0.006	$-0.65 \pm 0.31 \pm 0.22$ [13]

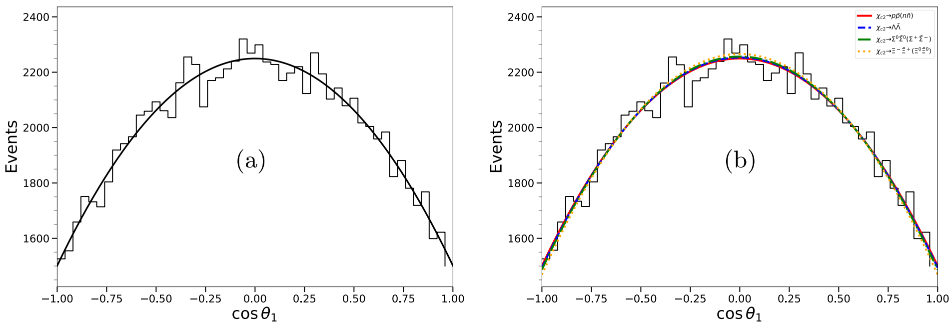

Fig. 3. (color online) Angular distributions of octet baryon in χ_{c1} (a) and χ_{c2} (b) decays. where histograms are MC events, and the curves are the expected distribution of $1-\alpha\cos^2\theta_1$ with $\alpha=-1/3$ (a) and $\alpha=0.333, 0.337, 0.341, 0.351$ for $p(n), \Lambda, \Sigma^0(\Sigma^+), \Xi^0(\Xi^-)$ (b).

channels. Based on the theoretical formula given in Eq. (10), we generate an ensemble of MC events and obtain the distribution for $\chi_{c1}\to B\bar{B}$ shown in Fig. 3(a). This remarkable universality makes the χ_{c1} decay a clean testbed for fundamental symmetries in QCD. For instance, the recent measured value by BESIII for $\chi_{c1}\to\Lambda\bar{\Lambda}$, $\alpha=-0.301\pm0.042\pm0.026$ [11], is in excellent agreement with this prediction, confirming the dominance of the helicity selection rule in this decay mode.

For the tensor state $\chi_{c2}\to B\bar{B}$, the situation is more complex. The angular distribution parameter α is also predicted to be negative, but its exact value is not universal; it depends on the relative magnitude and phase of two independent helicity amplitudes. These amplitudes are sensitive to the detailed dynamics of the decay, such as the wave function overlap and the spin structure of the final-state baryons, and thus can be calculated within specific frameworks like the quark model. We use the angular distribution formula in Eq. (12) and the parameter α fixed from the helicity amplitudes in Table 1, to generate an ensemble of MC events using an acceptance-rejection method for the χ_{c2} decays. Figure 3(b) shows the angular distribution for $\chi_{c2}\to B\bar{B}$, histogram is filled with the MC events, and the comparison with the predicted angular distribution (curve).

The angular distributions in different baryon channels ($p\bar{p}$, $\Lambda\bar{\Lambda}$, $\Sigma^0\bar{\Sigma}^0(\Sigma^+\bar{\Sigma}^-)$, $\Xi^-\bar{\Xi}^+(\Xi^0\bar{\Xi}^0)$) exhibit subtle yet discernible differences in the Fig. 3, reflecting the dependence of the decay amplitudes on the flavor structure of the final-state baryons. Current experimental measurements for χ_{c2} decays into $p\bar{p}$, $\Lambda\bar{\Lambda}$ and $\Xi^-\bar{\Xi}^+$ ($\Xi^0\bar{\Xi}^0$) all yield negative α values [9, 11, 13], and the results are consistent with quark-model calculations within one standard deviation. To more stringently test these theoretical predictions and decode the intricate decay mechanisms of χ_{cJ} states, future high-statistics experiments are crucial. Improving the precision of existing measurements and performing the first measurement for the $\chi_{c2}\to\Sigma^0\bar{\Sigma}^0$ channel will provide essential data. These precise determinations of α across the baryon octet will serve as critical benchmarks, allowing us to distinguish between different model assumptions and ultimately achieve a deeper understanding of the interplay between perturbative and non-perturbative QCD in charmonium decays.

B. Baryonic polarization and spin correlation

In the decay $\chi_{c0}\to B\bar{B}$, the parent particle's zero spin forbids any net polarization of the final-state baryons along any axis (x, y, or z). However, the spins of the baryon and antibaryon remain strongly quantum correlated. These non-classical spin correlations, a signature of entanglement, are not directly visible in the primary decay products. They can, however, be observed through momentum-angle correlations among the particles from the subsequent weak decays of both the baryon and antibaryon.

For the process $\chi_{c1}\to B\bar{B}$, the initial longitudinal polarization of the colliding beams is transferred to the χ_{c1} and manifests as a longitudinal polarization of the final-state baryon and antibaryon. This polarization is directly measurable. Furthermore, the spin correlations between the baryon pair are encoded in their joint angular distribution, specifically in the dependence on the polar angle θ_1, allowing for a complete analysis of the spin state from the primary decay vertex.

Figure 4 presents the longitudinal polarization components O_z and $\bar{O}_z$ of the baryon and antibaryon as functions of $\cos\theta_1$ in these decays. In all channels, $O_z(\bar{O}_z)$ is found to be consistent with zero, in agreement with the suppression of longitudinal polarization expected from helicity conservation in pseudovector meson decays. Figure 5 shows that the distributions of the spin correlation matrix elements in these decays are consistent across different baryon channels, indicating that the spin correlation pattern in χ_{c1} decays is primarily governed by the symmetry of the initial state and exhibits negligible dependence on the flavor structure of the final-state baryons.

The decay $\chi_{c2}\to B\bar{B}$ yields a different polarization pattern. Here, the baryon and antibaryon possess only a non-zero transverse polarization along the y-axis (perpen-

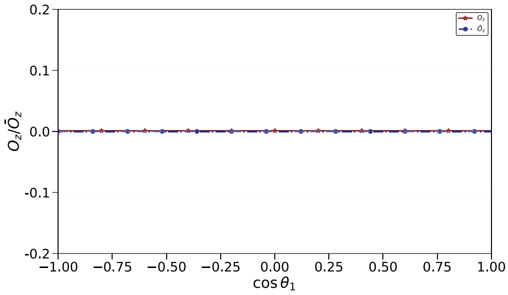

Fig. 4. (color online) The dependence of the polarizations O_z and $\bar{O}_z$ on $\cos\theta_1$ for the baryon and antibaryon in $\chi_{c1}\to B\bar{B}$ (B: octet baryon).

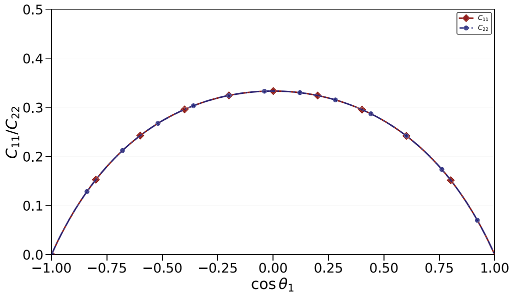

Fig. 5. (color online) The dependence of spin correlation matrix elements C_{ij} on $\cos\theta_1$ in $\chi_{c1}\to B\bar{B}$ (B: octet baryon).

dicular to the production plane). The magnitude of this transverse polarization depends on the ratio and relative phase between the two independent helicity amplitudes governing the decay. As in the χ_{c1} case, the spin correlations between the pair are also embedded in and can be extracted from the polar angular distribution $I(\cos\theta_1)$.

Based on Eq. (17) to Eq. (22) and the helicity amplitude values derived from the naive quark model in Table 1, the transverse polarization and the spin correlation matrix for the process$\chi_{c2}\to B\bar{B}$ can be obtained under the assumption of quark masses and energies. The phase angle Δ can only be determined by fitting to experimental data, such as the value $\Delta=-0.37\pm0.16$ provided by BESIII for the $\chi_{c2}\to\Lambda\bar{\Lambda}$ decay [11]. When predicting the polarization vector and spin correlation tensor, we set $\Delta=\pi/2$ and $\Delta=0$ in our simulations. As shown in Fig. 6, a non-zero transverse polarization O_y is observed in all decay channels, with its magnitude following a flavor-dependent pattern. Figure 7 shows the calculations of the spin correlation matrix C_{ij} in $\chi_{c2}\to B\bar{B}$ decays ($B=p$, $\Lambda,\Sigma^0(\Sigma^+),\Xi^-(\Xi^0)$). A strong longitudinal alignment ($C_{33}\approx1$) and universal transverse anisotropy ($C_{11}>C_{22}$) across all channels. The effect is most pronounced for $\Xi^-\bar{\Xi}^+(\Xi^0\bar{\Xi}^0)$, suggesting that interference among helicity amplitudes is modulated by baryon spin structure. These results link charmonium decay dynamics to flavor-dependent baryon structure.

VI. SUMMARY AND OUTLOOK

In this work, we have performed a comprehensive polarization analysis of χ_{cJ} ($J=0,1,2$) decays into spin-1/2 baryon-antibaryon pairs, with a focus on the novel scenario where the χ_{cJ} states are produced via polarized electron-positron collisions. Starting from the spin density matrix formalism, we systematically derived the polarization transfer from the initial beam to the intermediate $\psi(2S)$ and χ_{cJ} resonances, and finally to the baryonic fi-

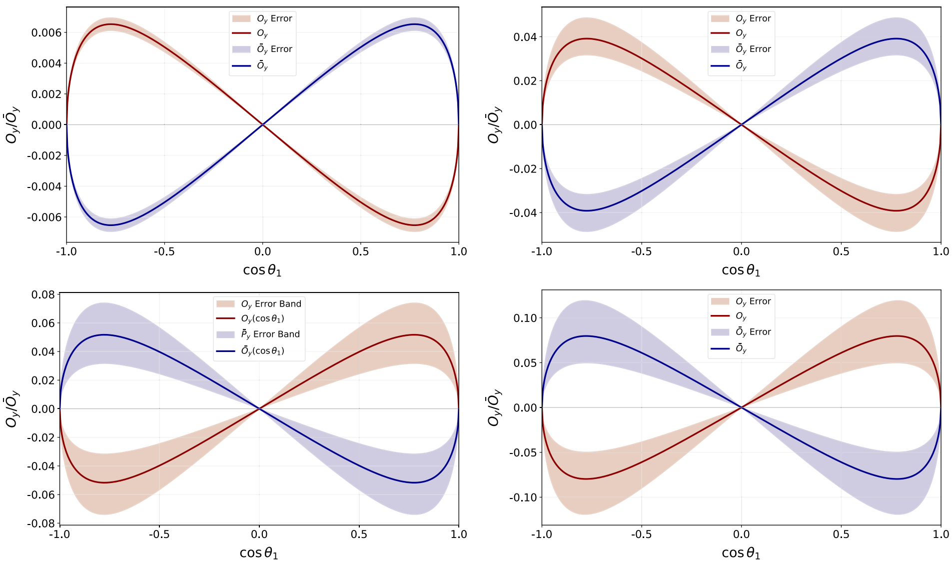

Fig. 6. (color online) The polarization components O_y and $\bar{O}_y$ of baryons and antibaryons from χ_{c2} decays are shown as follows: the upper-left panel corresponds to $p\bar{p}$ ($n\bar{n}$); the upper-right, to $\Lambda\bar{\Lambda}$; the bottom-left, to $\Sigma^0\bar{\Sigma}^0$ ($\Sigma^+\bar{\Sigma}^-$); and the bottom-right, to $\Xi^-\bar{\Xi}^+$ ($\Xi^0\bar{\Xi}^0$). The parameters b_{+-} and b_{++} are taken from the numerical values in Table 1. The solid line corresponds to their central values, and the shaded band indicates the uncertainties.

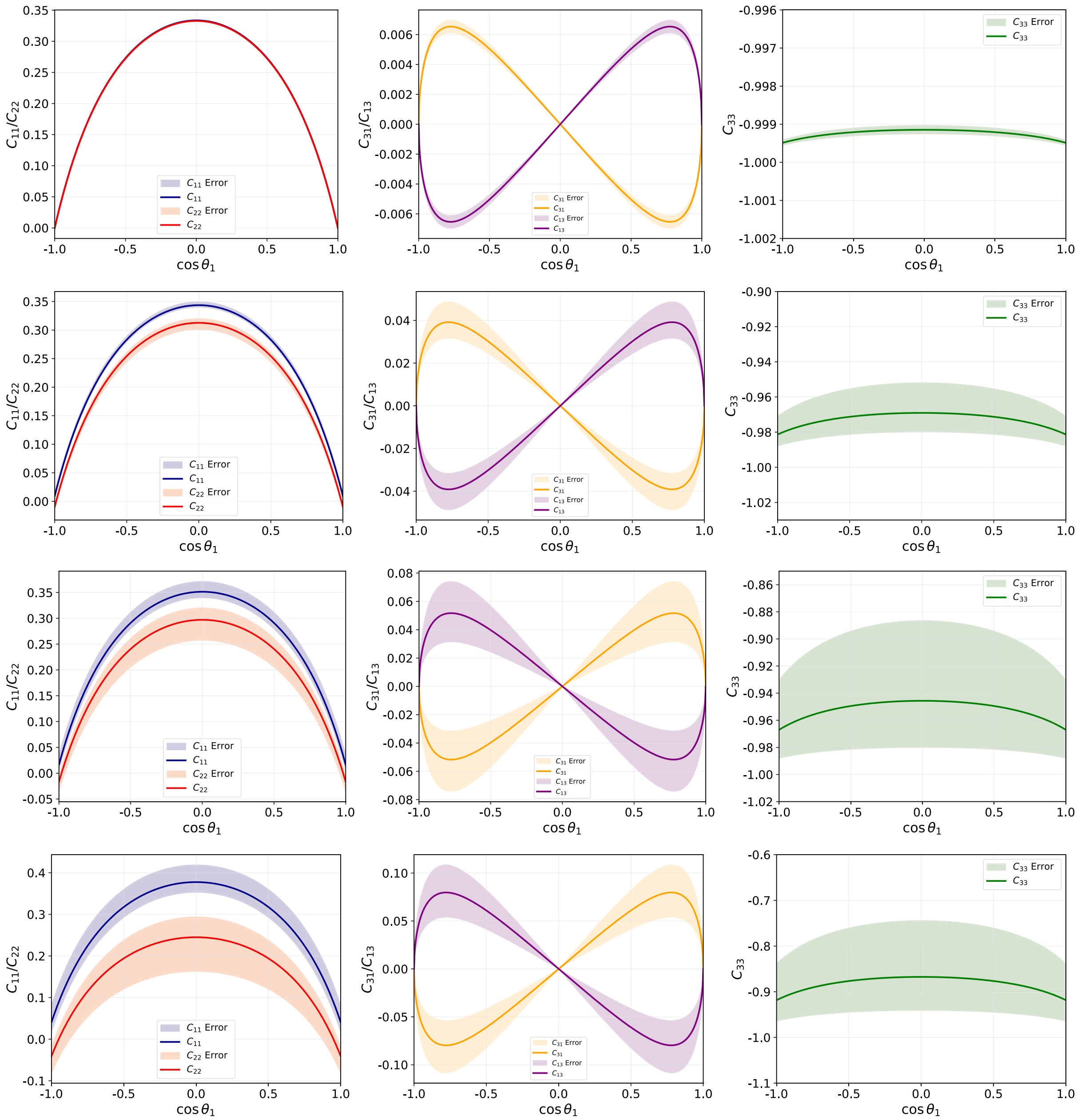

Fig. 7. (color online) The spin correlation matrix elements C_{ij}. The first row corresponds to $\chi_{c2} \to p\bar{p}$, the second to $\chi_{c2} \to \Lambda\bar{\Lambda}$, the third to $\chi_{c2} \to \Sigma^0\bar{\Sigma}^0$, and the fourth to $\chi_{c2} \to \Xi^-\bar{\Xi}^+$ ($\Xi^0\bar{\Xi}^0$). The parameters b_{+-} and b_{++} are set to the numerical values in Table 1. The solid line uses their central values, and the shaded band denotes the uncertainties.

nal states. For the subsequent decay $\chi_{cJ} \to B\bar{B}$, we calculated the complete set of helicity amplitudes within a constituent quark model framework, incorporating the full $SU(6)$ spin-flavor wave functions for octet baryons.

Our key findings can be summarized as follows. First, the angular distribution parameter α for $\chi_{c1} \to B\bar{B}$ is confirmed to be universally $-1/3$, a robust prediction arising from the helicity selection rule imposed by charge-conjugation symmetry. Second, in the case of χ_{c2} decays, the α parameter, the transverse polarization along the y-axis, and the spin correlation tensor all depend on the ratio and relative phase of two independent helicity amplitudes. Our calculated results are consistent with available experimental measurements within the quoted uncertainties. Finally, under a polarized beam scenario, the initial longitudinal beam polarization P_z modifies the spin density matrices of χ_{c1} and χ_{c2}, which induces observable effects in the final-state baryon polarizations and spin correlations. By contrast, the decay of χ_{c0} remains insensitive to beam polarization.

Looking forward, our work provides a theoretical toolkit for future experiments utilizing polarized beams, such as the proposed STCF. Measurements of the detailed angular distributions and spin correlations with polarized e^+e^- collisions will offer unprecedented precision to test the quark model calculations, scrutinize the helicity selection rules, and probe potential contributions beyond the dominant E1 transition. Furthermore, the predicted strong spin entanglement in χ_{c0} decays and the polarization-dependent entanglement witness in $\chi_{c1,2}$ decays open a promising avenue to explore quantum entanglement in high-energy physics, potentially using these processes as a sensitive probe for new physics beyond the Standard Model.

APPENDIX A: SPIN WAVE FUNCTION OF χ_{c2}

The spin wave functions of χ_{c2} in its rest frame are taken

$$\begin{aligned}
\epsilon_{\mu\nu}(0) &= \frac{1}{\sqrt{6}}(\epsilon_\mu(1)\epsilon_\nu(-1)+2\epsilon_\mu(0)\epsilon_\nu(0)+\epsilon_\mu(-1)\epsilon_\nu(1)),\\
\epsilon_{\mu\nu}(\pm1) &= \frac{1}{\sqrt{2}}(\epsilon_\mu(\pm1)\epsilon_\nu(0)+\epsilon_\mu(0)\epsilon_\nu(\pm1)),\\
\epsilon_{\mu\nu}(\pm2) &= \epsilon_\mu(\pm1)\epsilon_\nu(\pm1).
\end{aligned}\tag{A1}$$

Here, $\epsilon(\pm1)=\mp\frac{1}{\sqrt{2}}(0,1,\pm\mathrm{i},0)^T$ and $\epsilon(0)=(0,0,0,1)^T$.

APPENDIX B: BARYON WAVE FUNCTION

In the naive quark model, the wave functions are constructed as follows. For the proton and neutron, neglecting the mass difference between the u and d quarks allows their flavor-spin wave functions to be explicitly expressed within the $SU(6)$ group representation. Within this framework, the flavor wave functions of the proton and neutron are given by:

$$\begin{aligned}
&\phi_p^\rho = \frac{1}{\sqrt{2}}(udu-duu),\quad \phi_n^\rho = \frac{1}{\sqrt{2}}(udd-dud),\\
&\phi_p^\lambda = -\frac{1}{\sqrt{6}}(duu+udu-2uud),\quad \phi_n^\lambda = \frac{1}{\sqrt{6}}(udd+dud-2ddu),
\end{aligned}\tag{B1}$$

where $\phi_{p,n}^\rho$ and $\phi_{p,n}^\lambda$ denote the antisymmetric and symmetric flavor wave functions of the proton and neutron, respectively. The overall flavor wave function exhibits mixed symmetry. The spin wave function of the spin-1/2 state with spin projection $\lambda=1/2$ is given as follows:

$$\begin{aligned}
\chi^\rho_{\frac{1}{2}} &= \frac{1}{\sqrt{2}}(|\uparrow\downarrow\uparrow\rangle-|\downarrow\uparrow\uparrow\rangle),\\
\chi^\lambda_{\frac{1}{2}} &= -\frac{1}{\sqrt{6}}(|\downarrow\uparrow\uparrow\rangle+|\uparrow\downarrow\uparrow\rangle-2|\uparrow\uparrow\downarrow\rangle).
\end{aligned}\tag{B2}$$

For the proton and neutron, the total spin-flavor wave function reads $\Psi_p=\frac{1}{\sqrt{2}}(\chi^\rho\phi^\rho+\chi^\lambda\phi^\lambda)$.

For the octet baryons (Λ,Σ,Ξ), the flavor wave functions are taken

$$\begin{aligned}
\phi_\Lambda &= \frac{1}{\sqrt{2}}(uds-dus),\\
\phi_{\Sigma^0} &= \frac{1}{\sqrt{2}}(uds+dus),\\
\phi_{\Sigma^+} &= uus,\\
\phi_{\Xi^{0,-}} &= ssu, ssd.
\end{aligned}\tag{B3}$$

The spin wave function for the spin 1/2 states with z-projection $\lambda=1/2$

$$\begin{aligned}
\chi_\Lambda &= \frac{1}{\sqrt{2}}(|\uparrow\downarrow\uparrow\rangle-|\downarrow\uparrow\uparrow\rangle),\\
\chi_{\Sigma^{0,+}} &= \frac{1}{\sqrt{6}}(|\uparrow\downarrow\uparrow\rangle+|\downarrow\uparrow\uparrow\rangle-2|\uparrow\uparrow\downarrow\rangle),\\
\chi_{\Xi^{0,-}} &= \frac{1}{\sqrt{6}}(|\uparrow\downarrow\uparrow\rangle+|\downarrow\uparrow\uparrow\rangle-2|\uparrow\uparrow\downarrow\rangle).
\end{aligned}\tag{B4}$$

Thus the wave functions are constructed as $\Psi_Y=\phi_Y\chi_Y$ with $Y=\Lambda,\Sigma^0(\Sigma^+)$ and $\Xi^0(\Xi^-)$.

References

[1] J. Bolz, P. Kroll, and G. A. Schuler, Eur. Phys. J. C **2**, 705 (1998)
[2] B. Q. Ma, I. Schmidt, J. Soffer *et al.*, Phys. Rev. D **65**, 034004 (2002)
[3] X. H. Liu and Q. Zhao, J. Phys. G **38**, 035007 (2011)
[4] M. Ablikim *et al.* (BESIII Collaboration), Nature Phys. **15**, 631 (2019)
[5] E. Perotti, G. Fäldt, A. Kupsc *et al.*, Phys. Rev. D **99**(5), 056008 (2019)
[6] G. Moortgat Pick, T. Abe *et al.*, Phys. Rept. **460**, 131 (2008)
[7] Z. Zhang, T. b. Liu, R. G. Ping *et al.*, Phys. Rev. D **112**(9), 096012 (2025)
[8] M. Ablikim *et al.* (BESIII Collaboration), Phys. Rev. D **87**(3), 032007 (2013)
[9] M. Ablikim *et al.* (BESIII Collaboration), Phys. Rev. D **88**(11), 112001 (2013)

[10] J. Z. Bai *et al.* (BES Collaboration), Phys. Rev. D **67**, 112001 (2003)

[11] M. Ablikim *et al.* (BESIII Collaboration), (2025), arXiv: 2509.00289 [hep-ex]

[12] M. Ablikim *et al.* (BESIII Collaboration), Phys. Rev. D **101**, 092002 (2020)

[13] M. Ablikim *et al.* (BESIII Collaboration), JHEP **06**, 74 (2022)

[14] R. Horodecki, P. Horodecki, M. Horodecki *et al.*, Rev. Mod. Phys. **81**, 865 (2009)

[15] G. Adesso and F. Illuminati, J. Phys. A **40**, 7821 (2007)

[16] A. Bernal, P. Caban, and J. Rembieliński, Sci. Rep. **15**(1), 23410 (2025)

[17] P. C. Hong, R. G. Ping, and W. M. Song, Phys. Rev. D **113**(7), 076009 (2026)

[18] C. Li, X. Cao, A. Q. Guo *et al.*, (2026), arXiv: 2602.10398

[19] G. Aad *et al.* (ATLAS Collaboration), Nature **633**(8030), 542 (2024)

[20] A. J. Barr, M. Fabbrichesi, R. Floreanini *et al.*, Prog. Part. Nucl. Phys. **139**, 104134 (2024)

[21] Z. T. Dong, D. Gonçalves, K. Kong *et al.*, Phys. Rev. D **109**(11), 115023 (2024)

[22] M. Achasov *et al.*, Front. Phys. (Beijing) **19**(1), 14701 (2024)

[23] J. D. Jackson, Rev. Mod. Phys. **48**, 417 (1976)

[24] X. Cao, Y. T. Liang, and R. G. Ping, Phys. Rev. D **110**(1), 014035 (2024)

[25] F. Tabakin and R. A. Eisenstein, Phys. Rev. C **31**, 1857 (1985)

[26] M. Ablikim *et al.* (BESIII Collaboration), Phys. Rev. D **84**, 092006 (2011)

[27] G. Karl, S. Meshkov, and J. L. Rosner, Phys. Rev. D **13**, 1203 (1976)

[28] H. Chen and R. G. Ping, Phys. Rev. D **102**, 016021 (2020)

[29] W. K. Wootters, Phys. Rev. Lett. **80**, 2245 (1998)

[30] R. G. Ping, B. S. Zou, and H. C. Chiang, Eur. Phys. J. A **23**, 129 (2004)

[31] R. G. Ping, H. C. Chiang, and B. S. Zou, Phys. Rev. D **66**, 054020 (2002)

[32] E. S. Ackleh, Ted Barnes, and E. S. Swanson, Phys. Rev. D **54**, 6811 (1996)

[33] S. Capstick and W. Roberts, Prog. Part. Nucl. Phys. **45**, S241 (2000)